

# PROPERTIES OF ISOSCALAR GIANT MULTIPOLE RESONANCES IN MEDIUM-MASS ONE-CLOSED-SHELL NUCLEI: A SEMI-MICROSCOPIC DESCRIPTION

M. L. Gorelik<sup>1</sup>, M. H. Urin<sup>2</sup>

<sup>1</sup>*Moscow Economic School, Moscow, Russia;*

<sup>2</sup>*National Research Nuclear University “MEPhI”, Moscow, Russia*

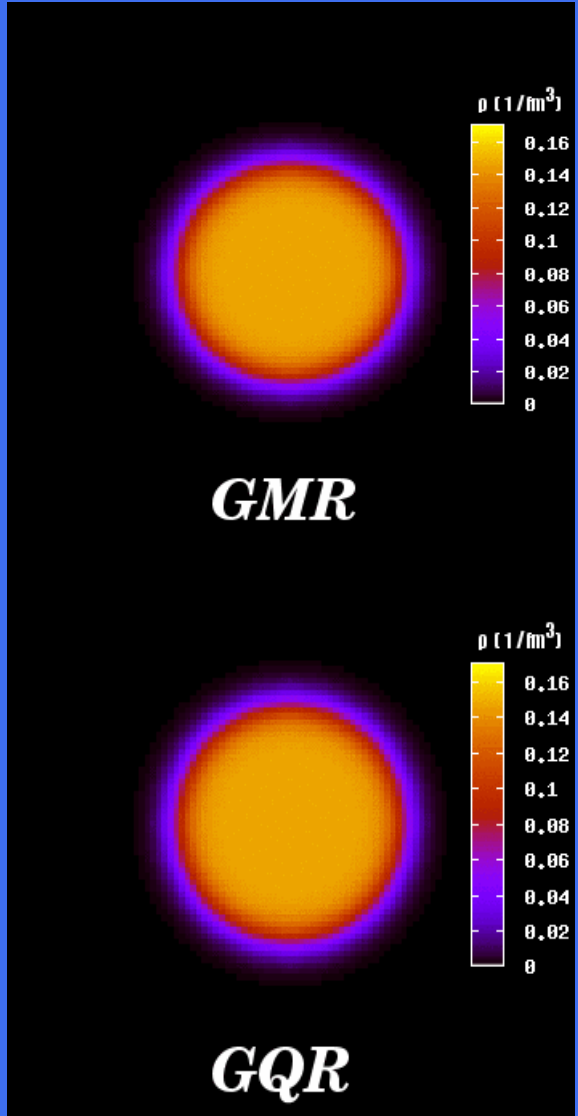
*Dedicated to memory of B.A. Tulupov*

Within the semi-microscopic particle-hole dispersive optical model, a description of the properties of the isoscalar giant multipole resonances in one-closed-shell nuclei is proposed. Some results are compared with experimental data obtained recently for the  $^{58}\text{Ni}$ ,  $^{120}\text{Sn}$ , and  $^{142}\text{Nd}$  nuclei.

1. Gorelik M.L., Shlomo S., Tulupov B.A., and Urin M.H. // Phys. Rev. C 2021. Vol. 103, P. 034302; Phys. Rev. C 2023. Vol. 108, P. 014328.
2. Bondarenko V.I. and Urin M.H. // Phys. Rev. C 2022. Vol. 106, P. 024331; Phys. Rev. C 2024. Vol. 109, P. 064610.
3. Abdullah M., Bagchi S., Harakeh M.N., et. al. // Phys. Lett. B 2024, Vol. 855, P. 138852.



# Isoscalar Giant Resonances

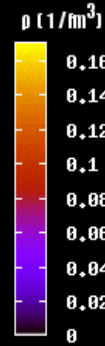
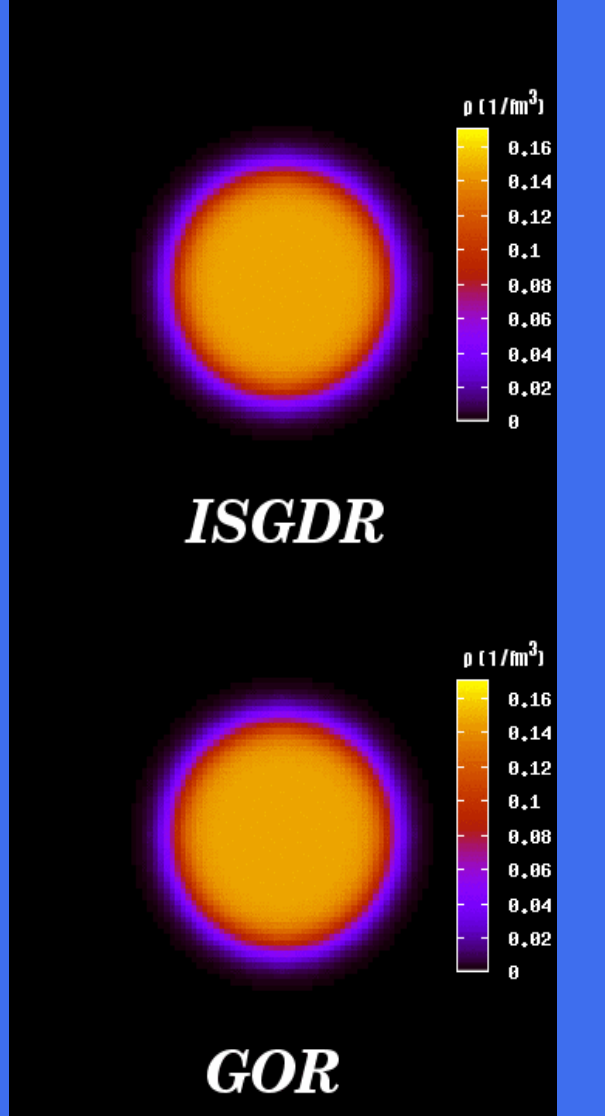


Breathing mode

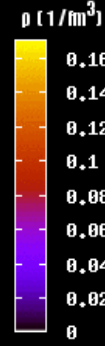
$$\sum r_i^2 \\ 2\hbar\omega$$

Squeezing mode

$$\sum r_i^3 Y_1 \\ 3\hbar\omega$$



**ISGDR**



**GOR**



## Ingredients of the model:

- (i) the Landau-Migdal p-h interaction;
- (ii) a phenomenological nuclear mean field partially consistent with interaction;
- (iii) the imaginary part of the effective optical model potential  
(this part determines the corresponding real part via a proper dispersive relationship).

Most of model parameters are taken from independent data, except of the intensity of the imaginary part, which is adjusted to reproduce in calculations the observable total width of the given giant resonance.



- the isospin symmetry of a model Hamiltonian

$$H_0 = \sum_a H_0(a)$$

$$F = \frac{1}{2} \sum_{a \neq b} F(a, b)$$

$$F(x_a, x_b) \rightarrow (F + F' \tau_a \tau_b) \delta(r_a - r_b)$$

The mean Coulomb  $U_C = \sum_a \frac{1}{2} \left(1 - \tau_a^{(3)}\right) U_C(r_a)$

- the main source of the weak violation of the isospin symmetry.

$$\begin{aligned} [H, T^{(-)}] &= U_C^{(-)} & U_C^{(-)} &= \sum_a U_C(a) \tau_a^{(-)} & U_1 &= \frac{1}{2} v(r) \tau^{(3)} \\ &\downarrow & &\downarrow & & \\ &RPA & &a & & \\ &\downarrow & & & & \\ & & & & n^{(-)}(r) &= n^n(r) - n^p(r) \end{aligned}$$

$$v(r) = 2F' n^{(-)}(r) \text{ - self-consistency condition}$$



- the translation symmetry of a model

$1^-$  spurious state

$$\omega \rightarrow 0 \quad EWSR \rightarrow 1$$

The Landau-Migdal particle-hole interaction

$$F(x, x') = C(F(r) + F' \tau \tau') \delta(r - r')$$

$$F(r) = f^{in} f_{WS}(r) + f^{ex}(1 - f_{WS}(r, R, a))$$

$$(EWSR)_{V_L} = \frac{\hbar^2}{2m} \int \left( \left( \frac{dV_L}{dr} \right)^2 + L(L+1) \left( \frac{V_L}{r} \right)^2 \right) n^{(+)}(r) r^2 dr$$



- The nuclear mean field

$$U(x) = U_0(x) + U_{so}(x) + U_1(x) + U_c(x)$$

$$U_0(x) = -U_0 f_{WS}(r, R, a)$$

$$U_{SO}(x) = -U_{SO} \frac{1}{r} \frac{df_{WS}}{dr} ls$$

$$U_1(x) = \frac{1}{2} v(r) \tau^{(3)}$$

$$U_c(x) = \frac{1-\tau^{(3)}}{2} U_c(r)$$



- SPREADING EFFECT – PHDOM

$[-iW(\omega) + P(\omega)]f_{WS}(r)$  - the "optical-model like" addition to the nuclear mean field

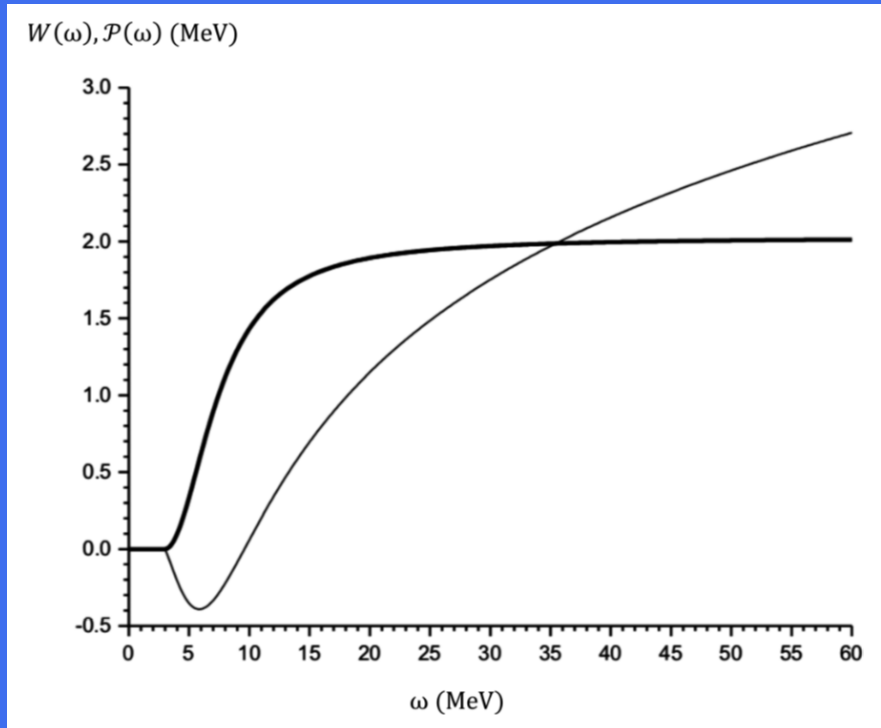
$$2W(\omega \geq \Delta) = \alpha \frac{(\omega - \Delta)^2}{1 + (\omega - \Delta)^2 / B^2},$$

$$W(\omega \leq \Delta) = 0$$

$$\alpha = 0.20 \text{ MeV}^{-1}$$

$$B = 4.5 \text{ MeV}$$

$$\Delta = 3.0 \text{ MeV}$$



- **Basic equations for describing high-energy isoscalar multipole excitations within the PHDOM**

Equation for the effective p-h propagator:

$$\widetilde{A}_L(r, r', \omega) = A_L(r, r', \omega) + \int A_L(r, r_1, \omega) \frac{F(r_1)}{r_1^2} \widetilde{A}_L(r_1, r', \omega) dr_1$$

$$\rho_L(r, r', \omega) = -\frac{1}{\pi} \text{Im } \widetilde{A}_L(r, r', \omega)$$

- double transition density

$$S_L(\omega) = -\frac{1}{\pi} \text{Im} \int V_L(r) \widetilde{A}_L(r, r', \omega) V_L(r') dr dr'$$

- strength function

$$S_L(\omega) = -\frac{1}{\pi} \text{Im} \int V_L(r) A_L(r, r', \omega) \widetilde{V}_L(r', \omega) dr dr'$$



- **Equation for the effective field:**

$$\widetilde{V}_L(r, \omega) = V_L(r) + \frac{F(r)}{r^2} \int A_L(r, r', \omega) \widetilde{V}_L(r', \omega) dr'$$

projected transition density

$$\rho_{V,L}(r, \omega) = \int \rho_L(r, r', \omega) V_L(r') dr' / S_L^{1/2}(\omega)$$

$$S_L(\omega) = \left( \int \rho_{V,L}(r, \omega) V_L(r) dr \right)^2$$

$$\frac{1}{r^2} \rho_{V,L}(r, \omega) = -\frac{1}{\pi} \text{Im} \frac{\widetilde{V}_L(r, \omega)}{F(r) S_L^{1/2}(\omega)}$$



- The IS radial component of the energy-averaged “free” p-h propagator

$$A_L(r, r', \omega) = A_L^i + A_L^{ii} + A_L^{iii}$$

$$A_L^i(r, r', \omega) = \sum_{(\lambda), \mu} n_\mu \left( t_{(\lambda)(\mu)}^L \right)^2 \chi_\mu(r) \chi_\mu(r') g_{(\lambda)}(r, r', \varepsilon_\mu + \omega)$$

$$A_L^{ii}(r, r', \omega) = \sum_{\lambda, (\mu)} n_\lambda \left( t_{(\lambda)(\mu)}^L \right)^2 \chi_\lambda(r) \chi_\lambda(r') g_{(\mu)}(r, r', \varepsilon_\mu - \omega)$$

$$A_L^{iii}(r, r', \omega) = \sum_{\lambda, \mu} n_\lambda n_\mu \left( t_{(\lambda)(\mu)}^L \right)^2 \chi_\lambda(r) \chi_\lambda(r') \chi_\mu(r) \chi_\mu(r') \times \\ \times \frac{2(iW(\omega) - P(\omega)) f_\lambda f_\mu}{(\varepsilon_\lambda - \varepsilon_\mu - \omega)^2 + (iW(\omega) - P(\omega))^2 f_\lambda^2 f_\mu^2}$$

$$t_{(\lambda)(\mu)}^L = \frac{1}{\sqrt{2L+1}} \langle (\lambda) | | Y_L | | (\mu) \rangle \quad f_\lambda = \int f_{WS}(r) \chi_\lambda^2(r) dr$$



## The optical-model radial Green functions satisfy to the equations:

$$\left[ h_{0,(\lambda)} - (\varepsilon_\mu + \omega + (iW(\omega) - P(\omega))f_\mu f_{WS}(r)) \right] \times \\ \times g_{(\lambda)}(r, r', \varepsilon_\mu + \omega) = -\delta(r - r')$$

$$\left[ h_{0,(\mu)} - (\varepsilon_\lambda - \omega + (iW(\omega) - P(\omega))f_\lambda f_{WS}(r')) \right] \times \\ \times g_{(\mu)}(r, r', \varepsilon_\lambda - \omega) = -\delta(r' - r)$$

$h_{0,(\lambda)}$   
 $h_{0,(\mu)}$

- are the radial parts of a s-p Hamiltonian (including the spin-orbit and centrifugal terms)



- Direct-one-nucleon-decay strength functions and branching ratios

$$S_{L,\mu}^{\uparrow}(\omega) = \sum_{(\lambda)} n_{\mu} \left( t_{(\lambda)(\mu)}^L \right)^2 \left| \int \chi_{\varepsilon_{\mu} + \omega, (\lambda)}^{*}(r) \widetilde{V}_L(r, \omega) \chi_{\mu}(r) dr \right|^2$$

$$S_L^{\uparrow}(\omega) = \sum_{\mu} S_{L,\mu}^{\uparrow}(\omega)$$

$$b_{L,\mu}^{\uparrow}(\omega_{12}) = \frac{\int_{\omega_1}^{\omega_2} S_{L,\mu}^{\uparrow}(\omega) d\omega}{\int_{\omega_1}^{\omega_2} S_L^{\uparrow}(\omega) d\omega} \quad - \text{the partial branching ratio}$$

$$b_{L,tot}^{\uparrow}(\omega_{12}) = \sum_{\mu} b_{L,\mu}^{\uparrow}(\omega_{12}) \quad - \text{the total branching ratio}$$



ЯДРО 2025

- Direct-one-nucleon-decay strength functions and branching ratios

$$S_{L,\mu}^{\uparrow}(\omega) = \sum_{(\lambda)} n_{\mu} \left( t_{(\lambda)(\mu)}^L \right)^2 \left| \int \chi_{\varepsilon_{\mu} + \omega, (\lambda)}^{*}(r) \widetilde{V}_L(r, \omega) \chi_{\mu}(r) dr \right|^2$$

$$S_L^{\uparrow}(\omega) = \sum_{\mu} S_{L,\mu}^{\uparrow}(\omega)$$

$$b_{L,\mu}^{\uparrow}(\omega_{12}) = \frac{\int_{\omega_1}^{\omega_2} S_{L,\mu}^{\uparrow}(\omega) d\omega}{\int_{\omega_1}^{\omega_2} S_L^{\uparrow}(\omega) d\omega}$$

- the partial branching ratio

$$b_{L,tot}^{\uparrow}(\omega_{12}) = \sum_{\mu} b_{L,\mu}^{\uparrow}(\omega_{12}) \quad - \text{the total branching ratio}$$

$$b_L^{\downarrow} = 1 - b_{L,tot}^{\uparrow}$$



- **Probing operators**

ISGMR     $V_{L=0}(r) = r^2 - \eta_0$

ISGQR     $V_{L=2}(r) = r^2$

ISGDR     $V_{L=1}(r) = r^3 - \eta_1 r$

$$\eta_1 \rightarrow \int V_{L=1}(r) \rho_{L=1}^{SS}(r) dr = 0 \quad \eta_1 \approx \frac{5}{3} \langle r^2 \rangle$$

ISGOR     $V_{L=3}(r) = r^3$

$$(EWSR)_{V_L} = \frac{\hbar^2}{2m} \int \left( \left( \frac{dV_L}{dr} \right)^2 + L(L+1) \left( \frac{V_L}{r} \right)^2 \right) n^{(+)}(r) r^2 dr$$

$$y_L(\omega) = \frac{\omega S_L(\omega)}{(EWSR)_{V_L}}$$



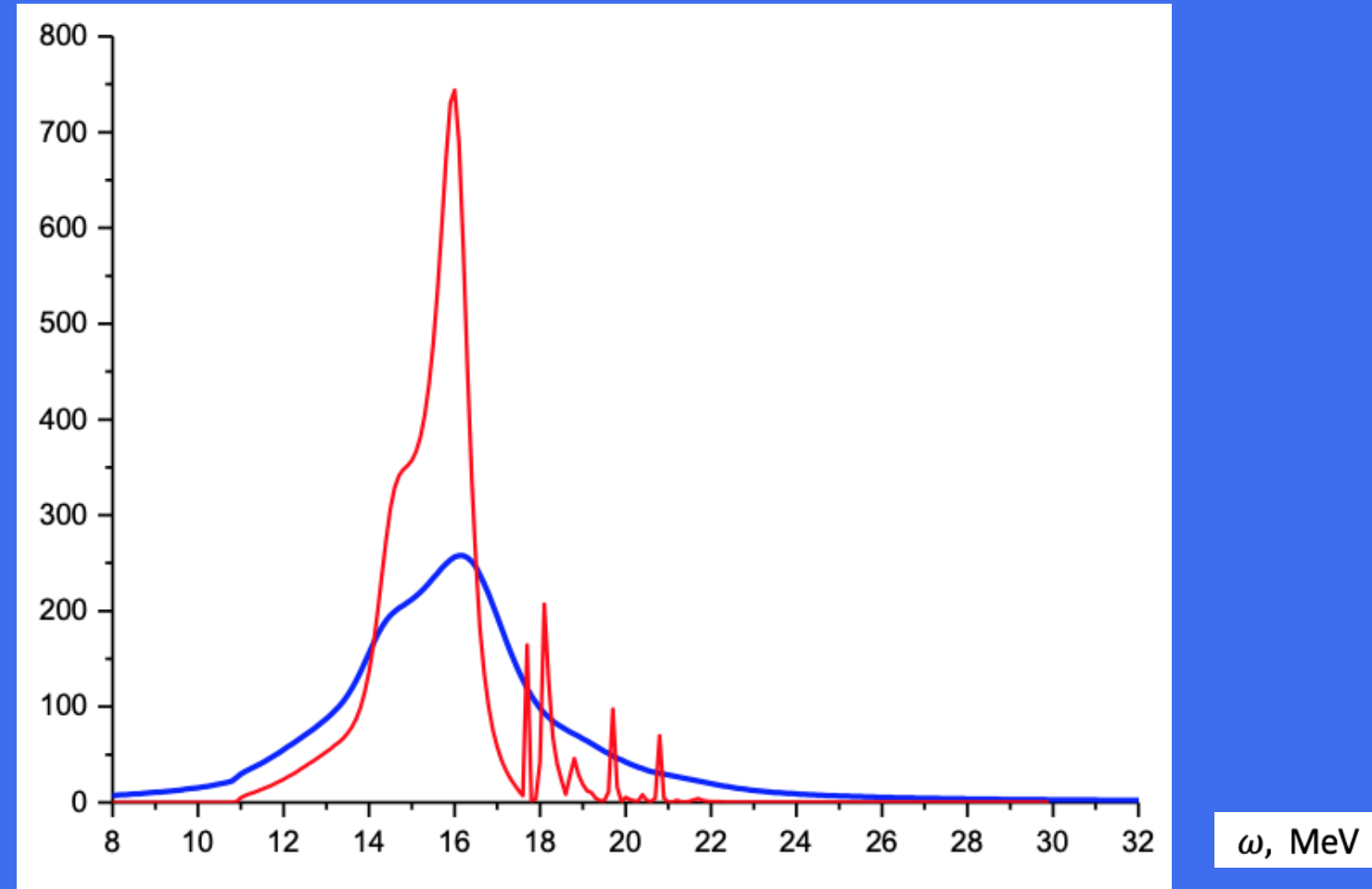
**Table 1. The mean-field and related model parameters used in PHDOM-based calculations of characteristics of ISGMPRS in nuclei under consideration.**

Nucleus	$U_0$ , MeV	$U_{ls}$ , MeV fm $^2$	$a$ , fm	$f'$	$-f^{ex}$
$^{48}\text{Ca}$	54.34	32.09	0.576	1.13	2.556
$^{58}\text{Ni}$	<b>54.49</b>	<b>32.93</b>	<b>0.586</b>	<b>1.11</b>	<b>2.564</b>
$^{90}\text{Zr}$	55.06	34.93	0.612	1.05	2.580
$^{120}\text{Sn}$	<b>55.38</b>	<b>35.86</b>	<b>0.629</b>	<b>1.01</b>	<b>2.610</b>
$^{132}\text{Sn}$	55.53	35.98	0.633	0.999	2.536
$^{142}\text{Nd}$	<b>55.66</b>	<b>35.97</b>	<b>0.636</b>	<b>0.991</b>	<b>2.568</b>
$^{208}\text{Pb}$	55.74	33.35	0.630	0.976	2.659

The values  $r_0 = 1.21$  fm and  $f^{\text{in}} = 0.0875$  are taken as universal quantities.



**Fig. 1. The strength functions calculated within cQRPA (red line) and PHDOM (blue line) for ISGMR in  $^{142}\text{Nd}$ .**



ЯДРО 2025

**Fig. 2. Fraction of the energy-weighted strength functions calculated for the ISGMR (blue line) and ISGMR2 (green line) in  $^{142}\text{Nd}$**

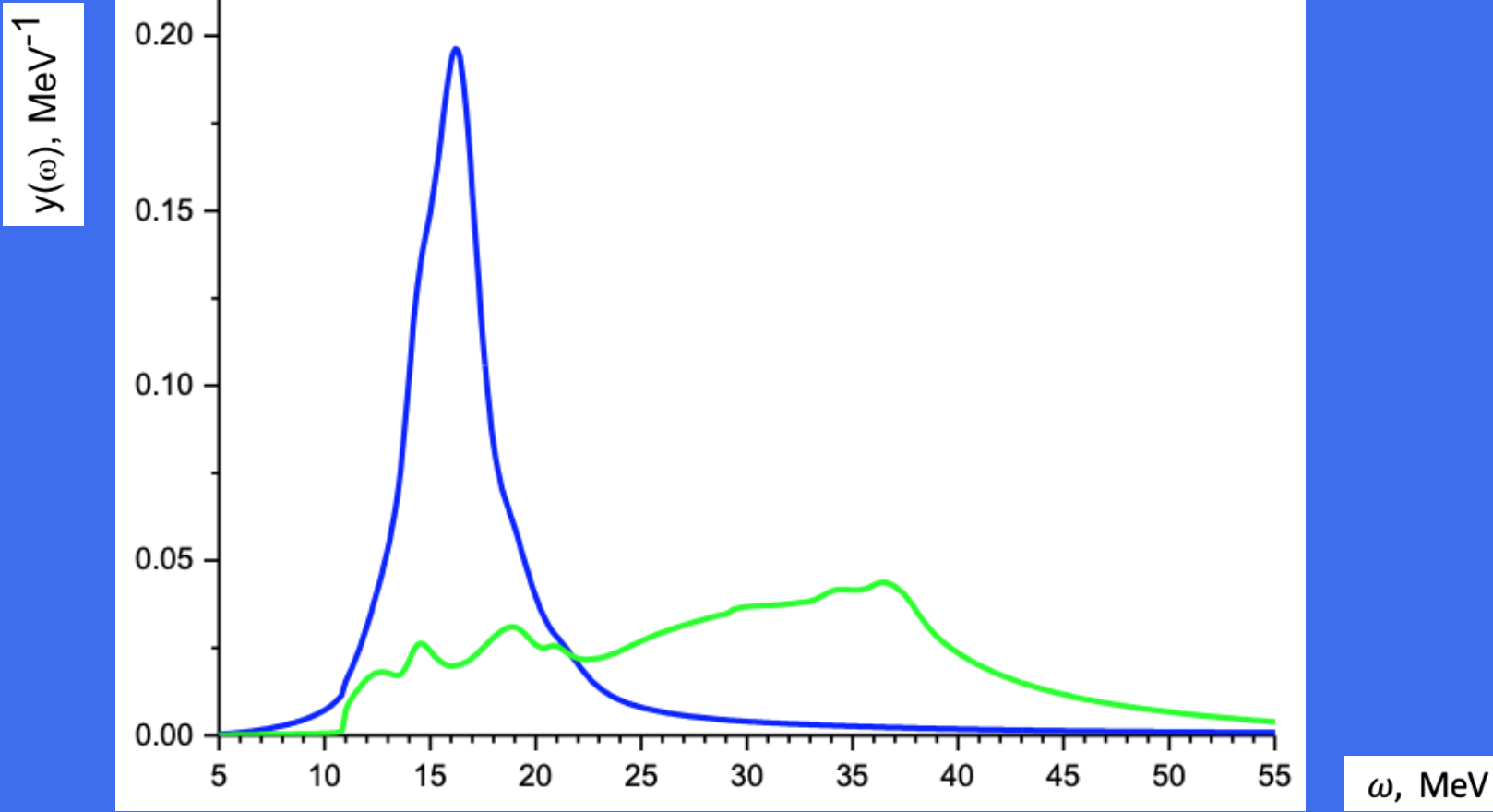


**Fig. 3. Fraction of the energy-weighted strength functions calculated for the ISGQR (blue line) and ISGQR2 (green line) in  $^{142}\text{Nd}$**

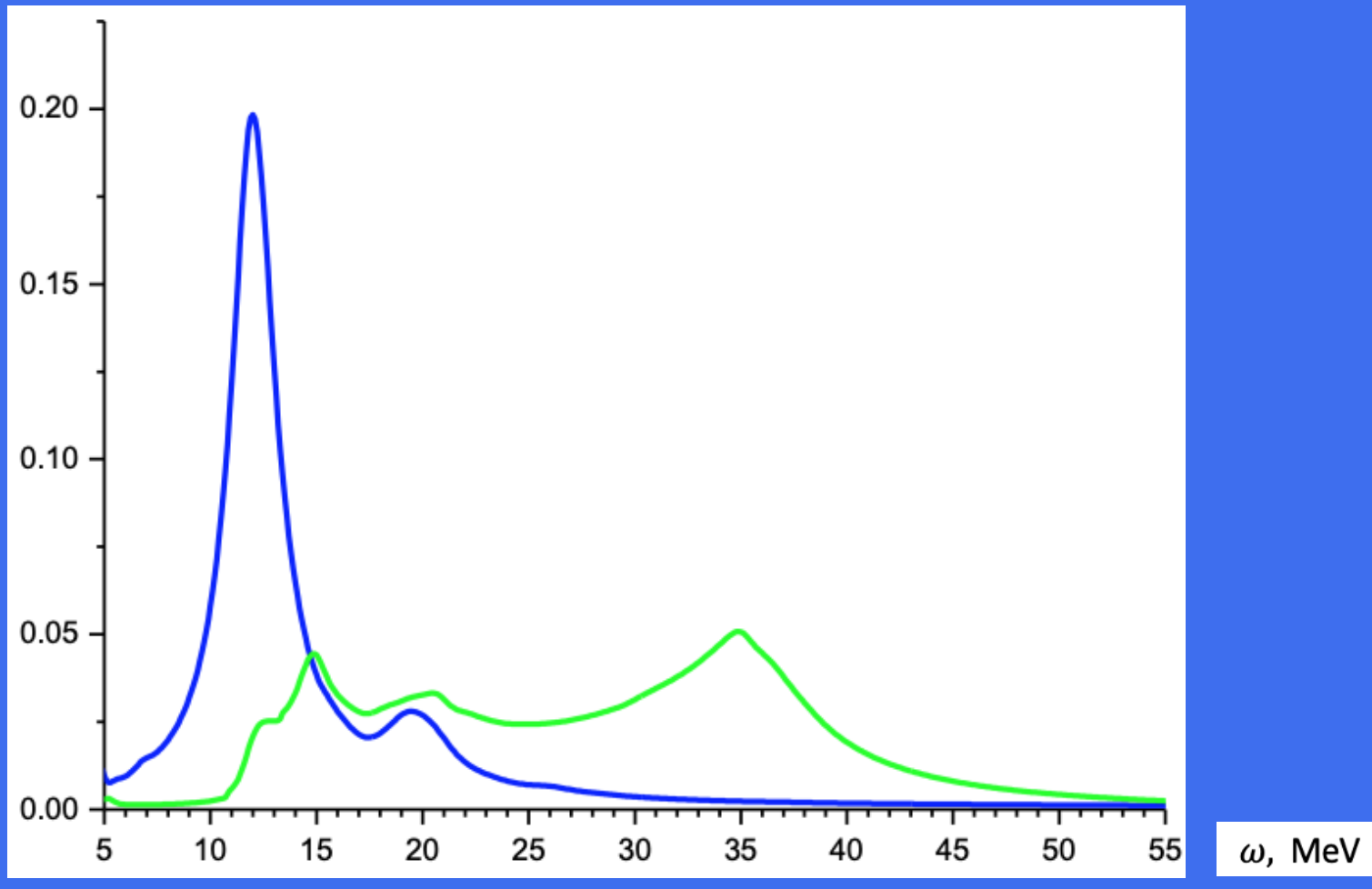
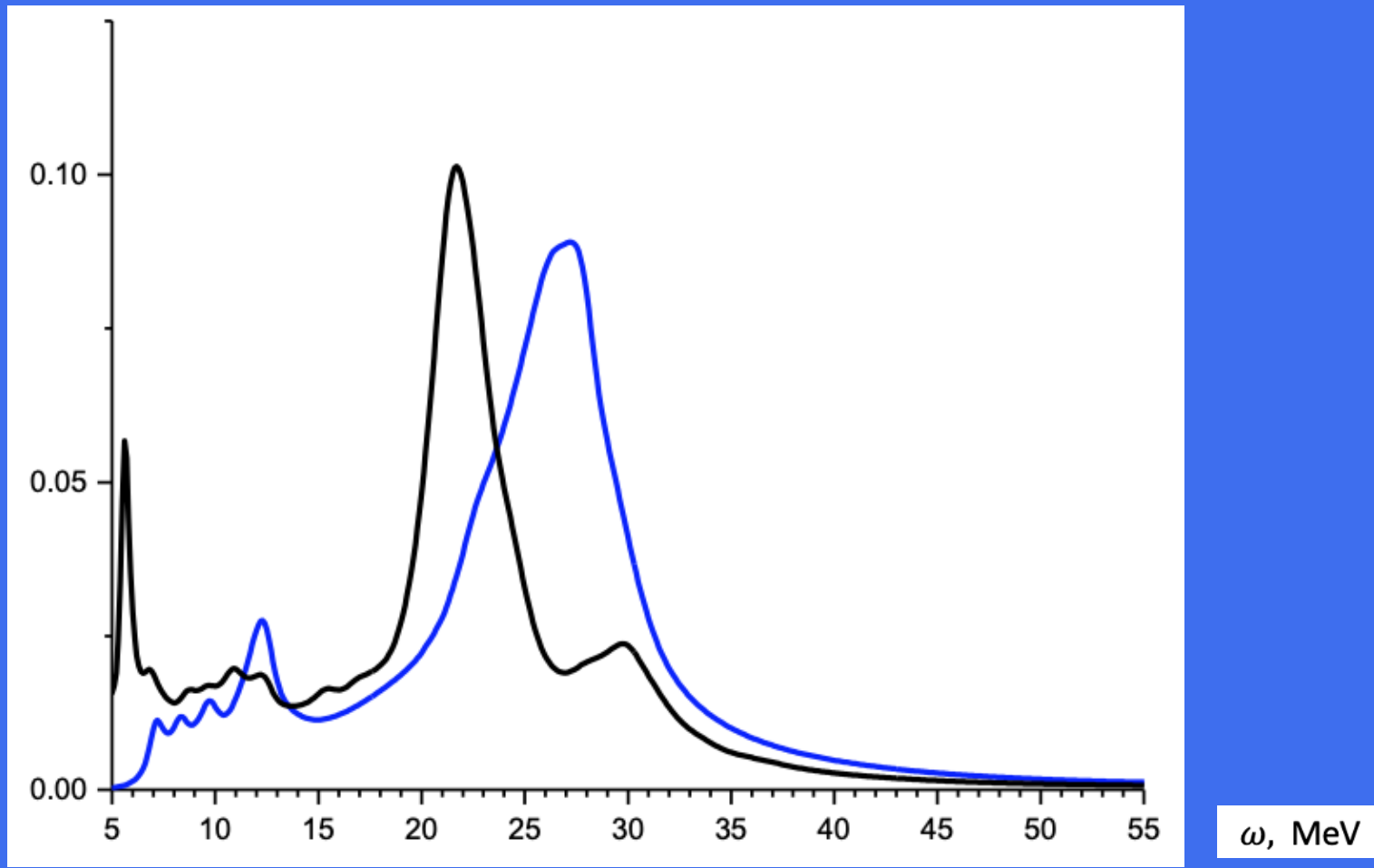


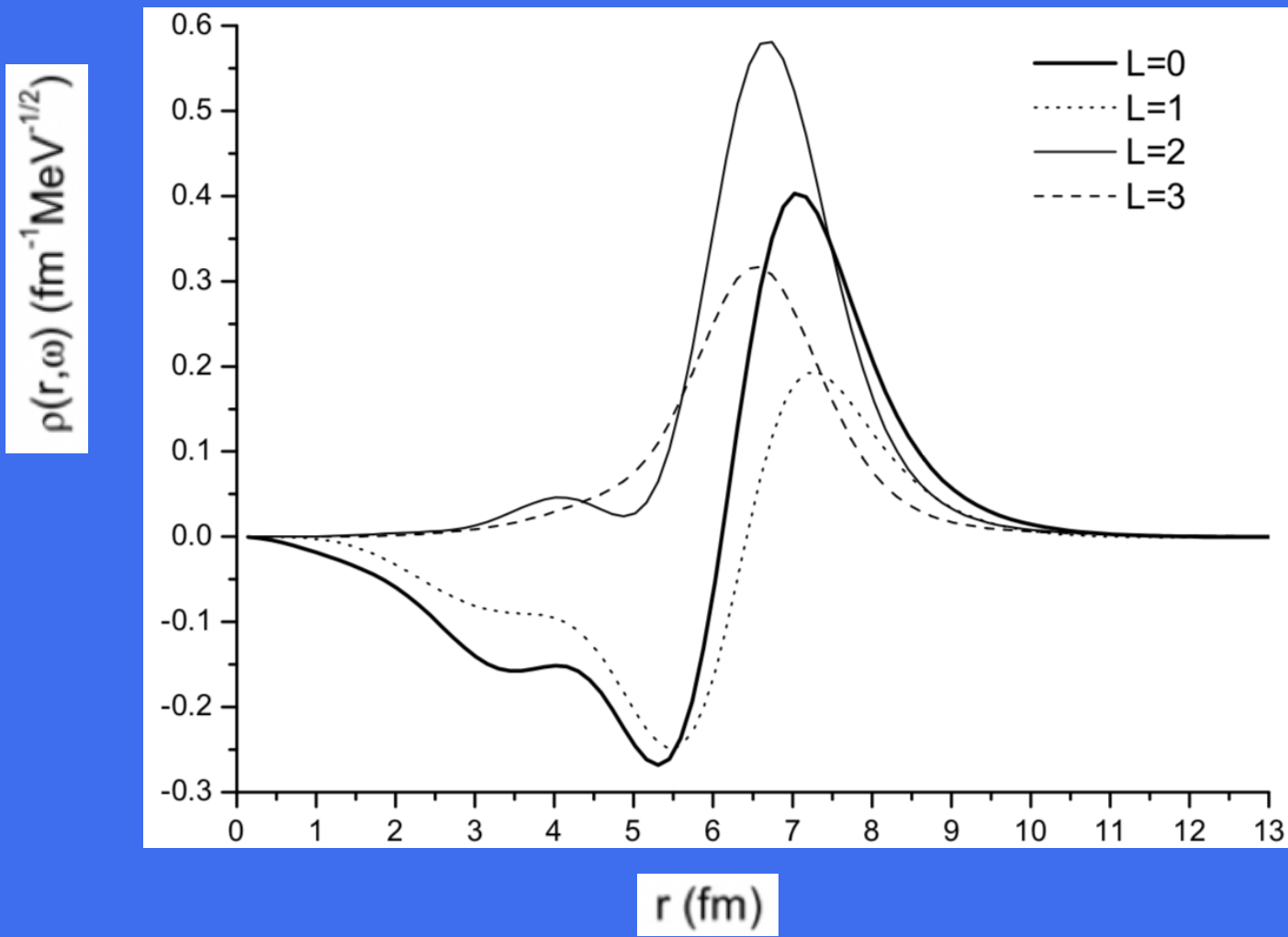
**Fig. 4. Fraction of the energy-weighted strength functions calculated for the ISGDR (blue line) and ISGOR (black line) in  $^{142}\text{Nd}$**



ЯДРО  
2025

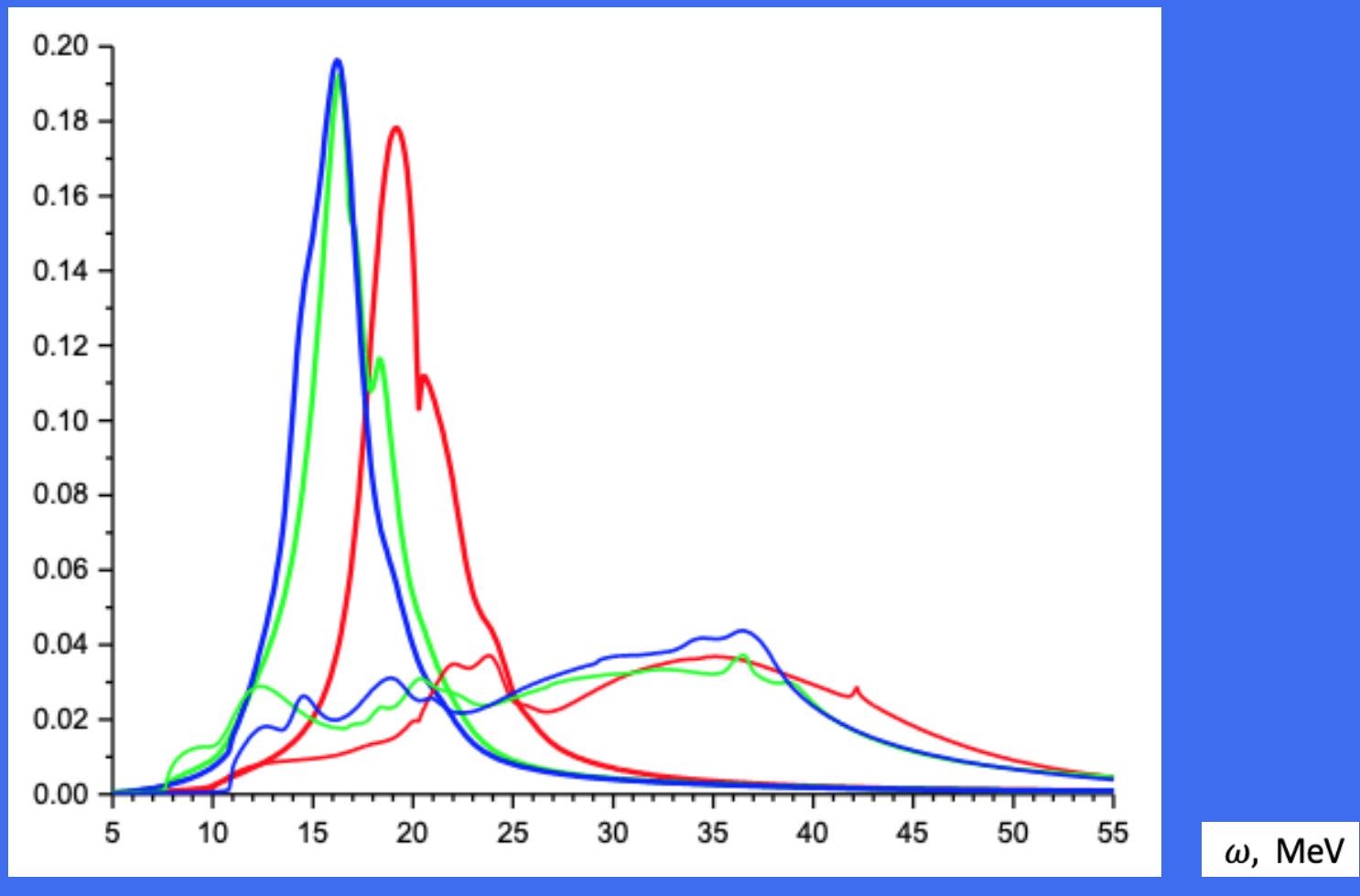


**Fig 5. Projected transition density calculated for the ISGRs in  $^{142}\text{Nd}$  at the energy of the main peak.**



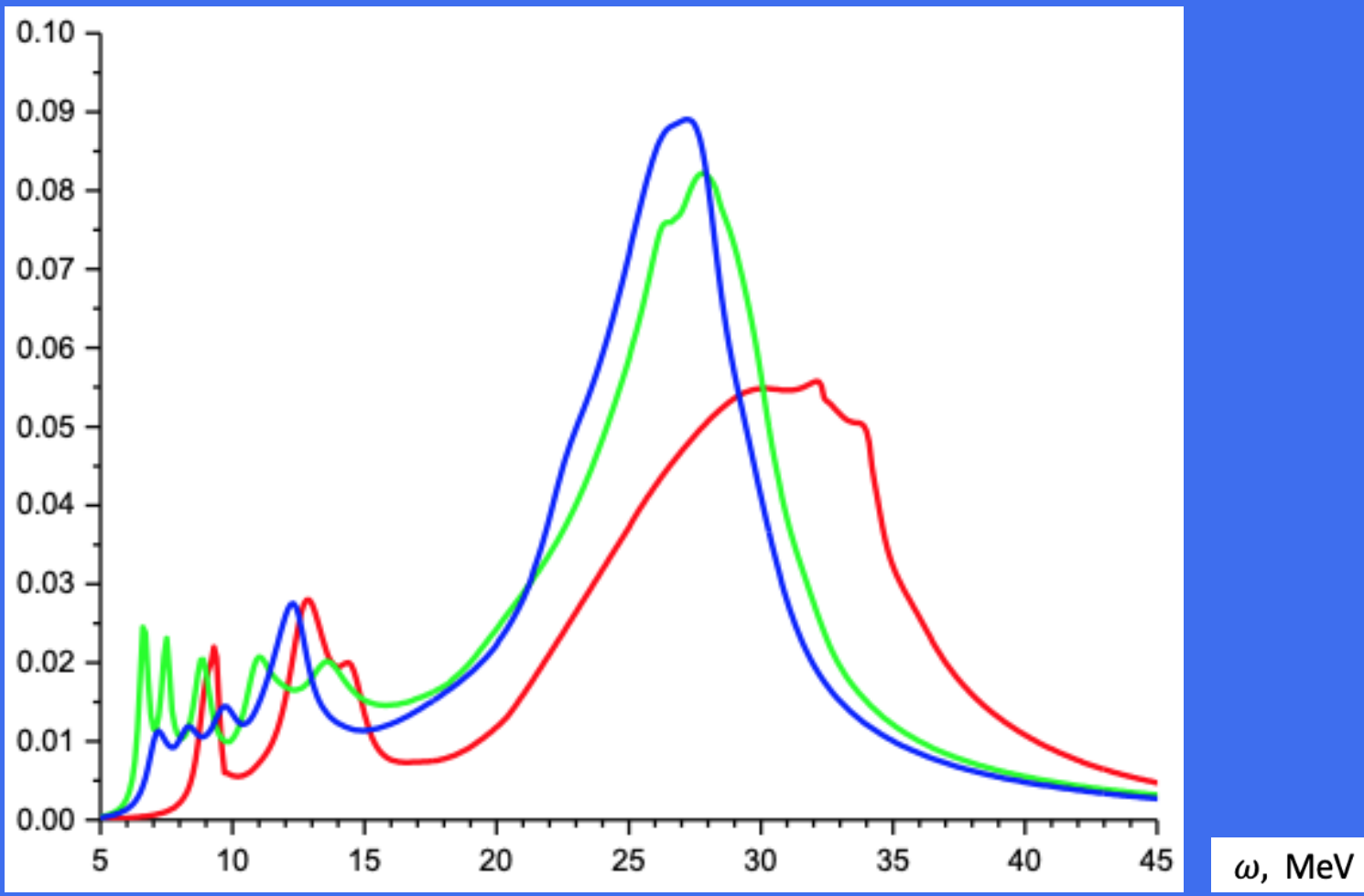
ЯДРО  
2025

**Fig. 6. Fraction of the energy-weighted strength functions calculated for the ISGMR (thick line) and ISGMR2 (thin line) in  $^{58}\text{Ni}$  (red),  $^{120}\text{Sn}$  (green),  $^{142}\text{Nd}$  (blue line).**



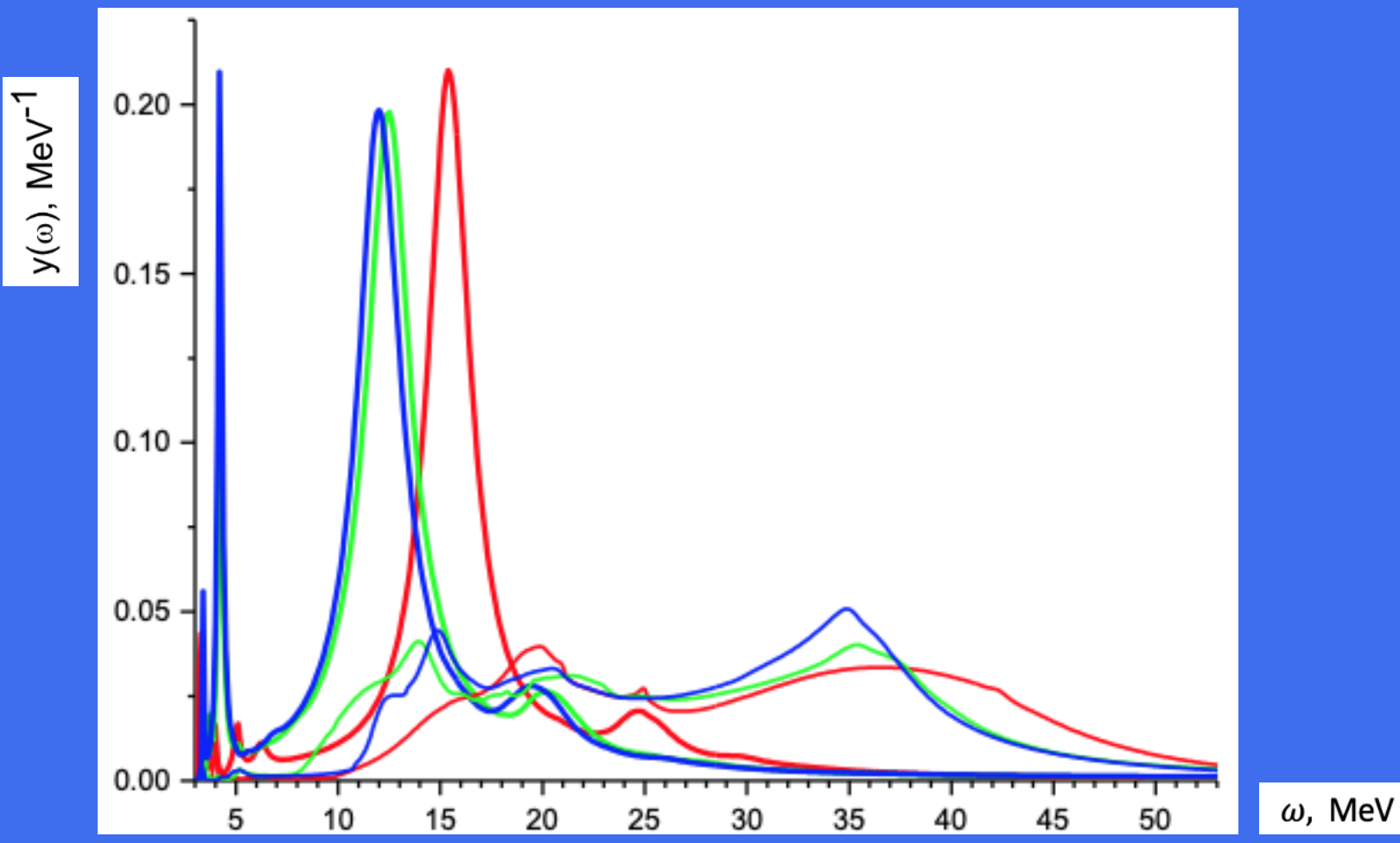
ЯДРО  
2025

**Fig. 7. Fraction of the energy-weighted strength functions calculated for the ISGDR in  $^{58}\text{Ni}$  (red),  $^{120}\text{Sn}$  (green),  $^{142}\text{Nd}$  (blue line).**



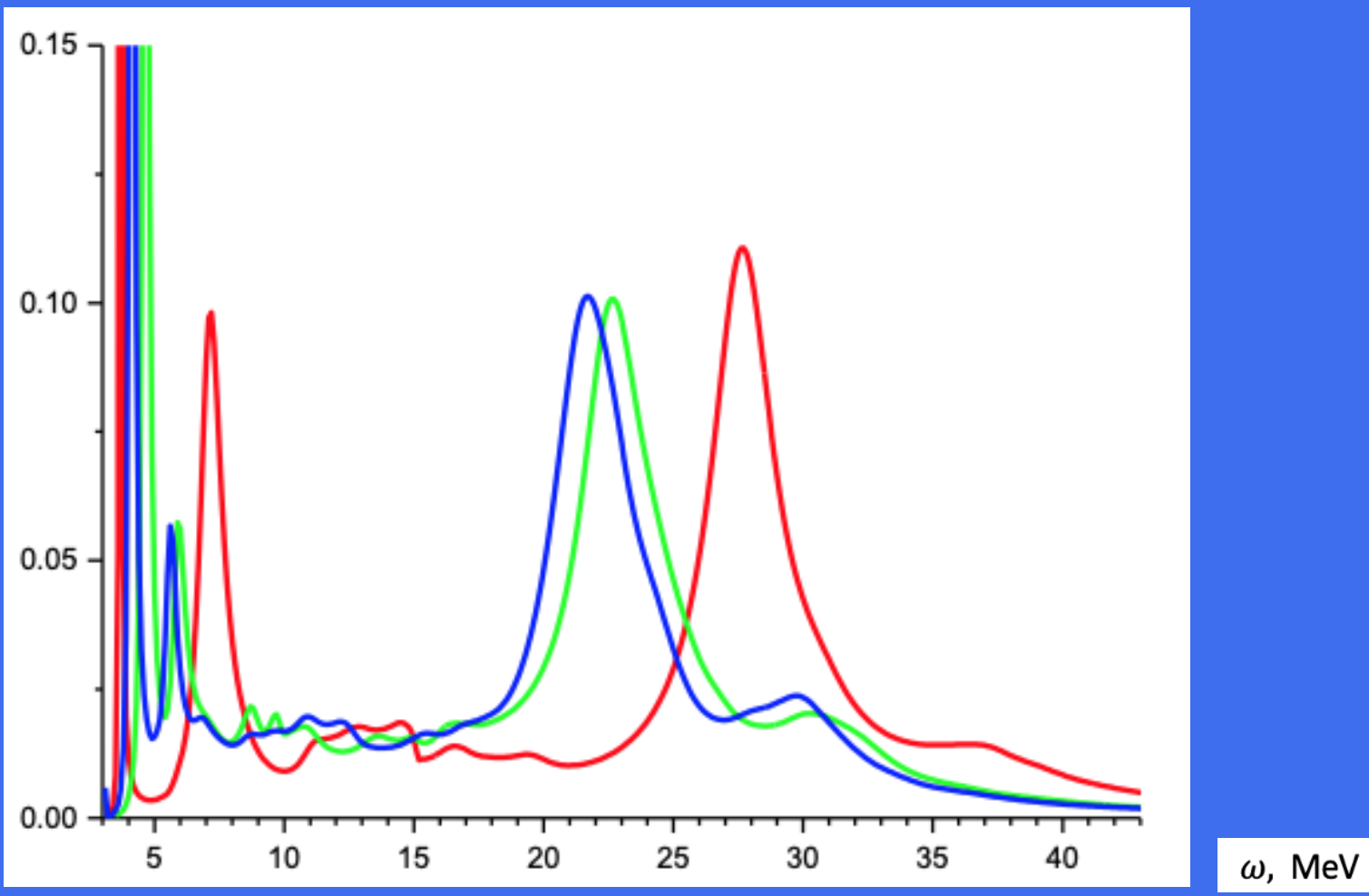
ЯДРО 2025

**Fig. 8. Fraction of the energy-weighted strength functions calculated for the ISGQR (thick line) and ISGQR2 (thin line) in  $^{58}\text{Ni}$  (red),  $^{120}\text{Sn}$  (green),  $^{142}\text{Nd}$  (blue line).**



ЯДРО  
2025

**Fig. 9. Fraction of the energy-weighted strength functions calculated for the ISGOR in  $^{58}\text{Ni}$  (red),  $^{120}\text{Sn}$  (green),  $^{58}\text{Ni}$  (blue line).**



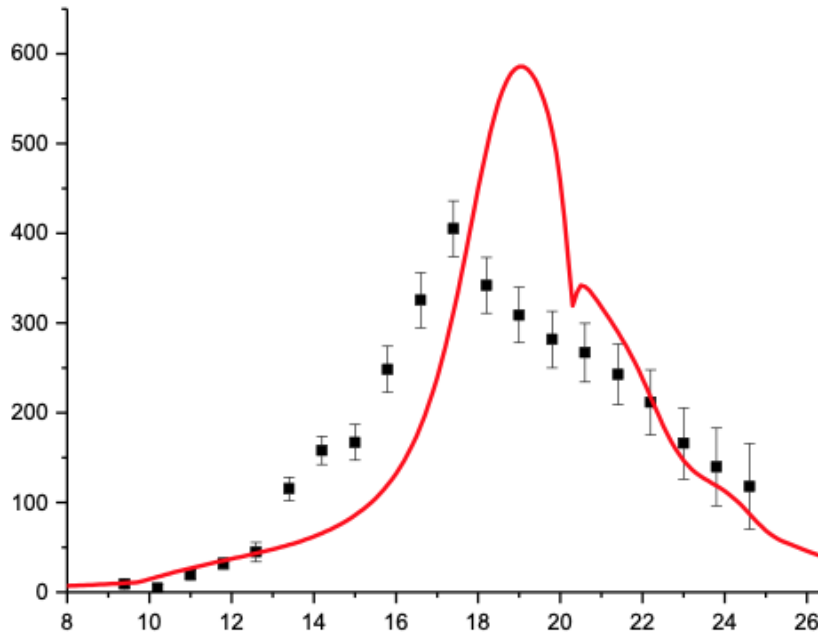
ЯДРО

2025

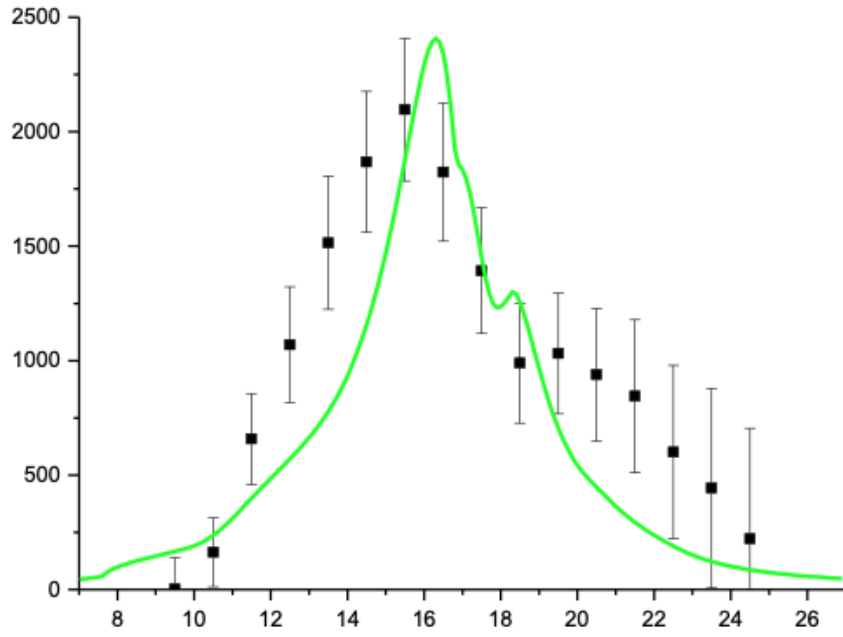
**Fig. 10. The strength functions  $S_L(\omega)$  evaluated within PHDOM for the ISGMR ( $L = 0$ ) in  $^{58}\text{Ni}$  (red),  $^{120}\text{Sn}$  (green line).**

$S_{L=0}(\omega)$  (fm $^4$  MeV $^{-1}$ )

$^{58}\text{Ni}$



$^{120}\text{Sn}$



$\omega$ , MeV



ЯДРО 2025

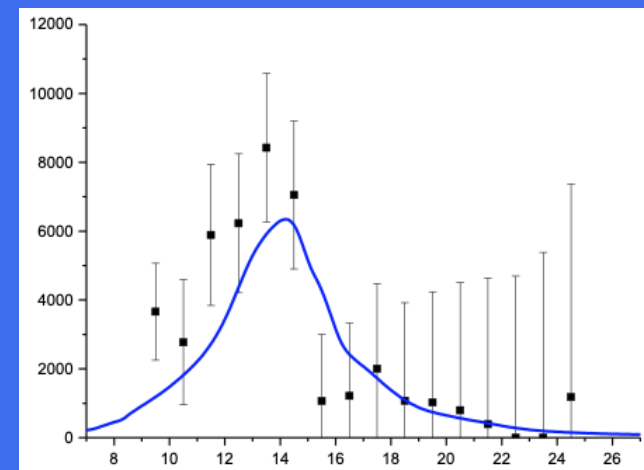
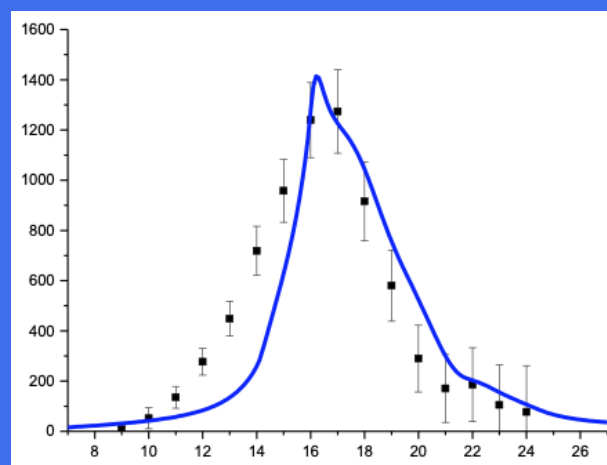
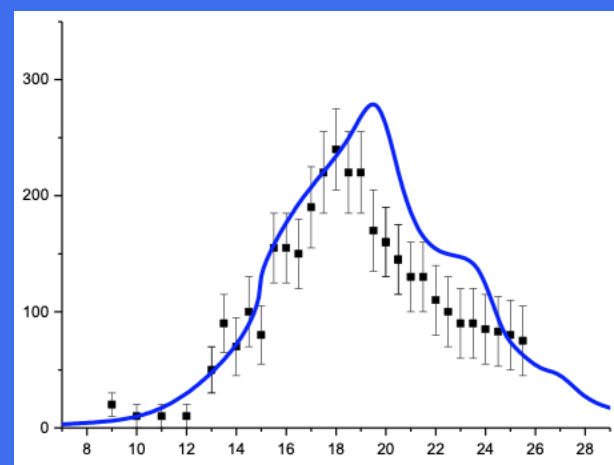
**Fig. 11. The strength functions  $S_L(\omega)$  evaluated within PHDOM for the ISGMR ( $L = 0$ ) in  $^{48}\text{Ca}$ ,  $^{90}\text{Zr}$ ,  $^{208}\text{Pb}$ .**

$S_{L=0}(\omega) (\text{fm}^4 \text{ MeV}^{-1})$

$^{48}\text{Ca}$

$^{90}\text{Zr}$

$^{208}\text{Pb}$



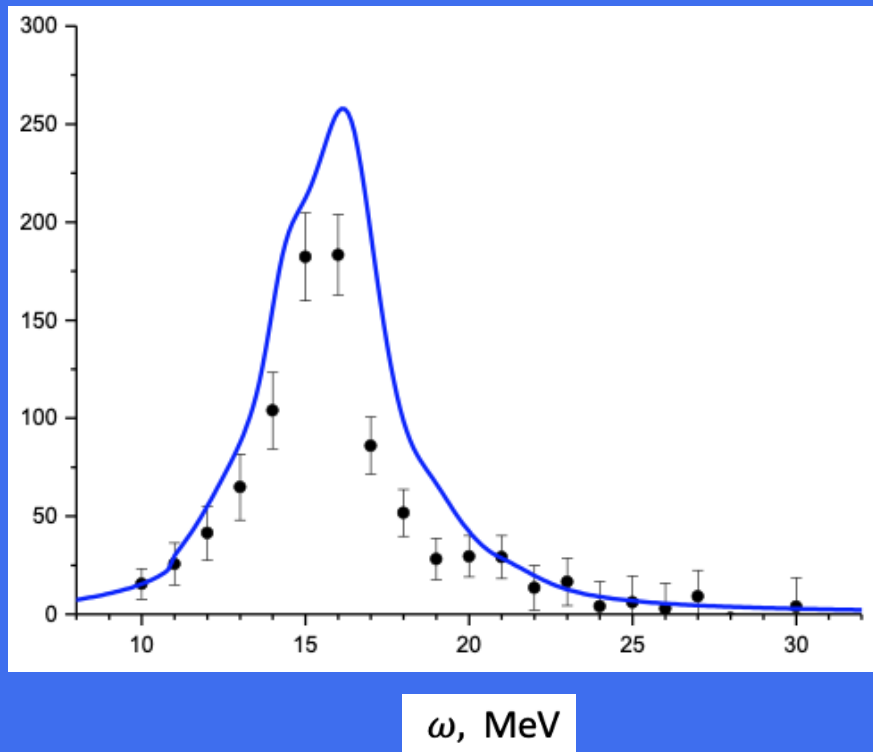
$\omega, \text{ MeV}$



2025

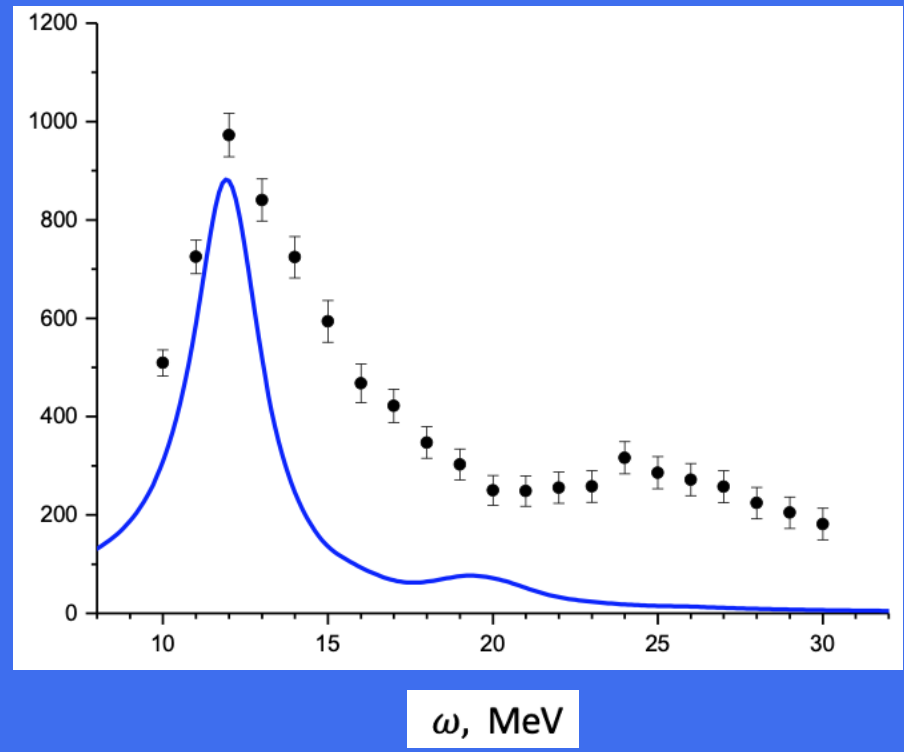
**Fig. 12. The strength functions  $S_L(\omega)$  evaluated within PHDOM for  $L = 0, 2$  GRs in  $^{142}\text{Nd}$  in a comparison with respective strength functions (multiplied by proper normalization factors) deduced from an analysis of respective reaction cross sections of GR excitation.**

$S_{L=0}(\omega) (\text{fm}^4 \text{ MeV}^{-1})$



$^{142}\text{Nd}$

$S_{L=2}(\omega) (\text{fm}^4 \text{ MeV}^{-1})$



$\omega$ , MeV

$\omega$ , MeV

Abdullah M., Bagchi S., Harakeh M.N., et. al. // Phys. Lett. B 2024, Vol. 855, P. 138852.



# PROPERTIES OF ISOSCALAR GIANT MULTIPOLE RESONANCES IN MEDIUM-MASS ONE-CLOSED-SHELL NUCLEI: A SEMI-MICROSCOPIC DESCRIPTION

M. L. Gorelik<sup>1</sup>, M. H. Urin<sup>2</sup>



<sup>1</sup>*Moscow Economic School, Moscow, Russia;*

<sup>2</sup>*National Research Nuclear University “MEPhI”, Moscow, Russia*

*Dedicated to memory of B.A. Tulupov*

Within the semi-microscopic particle-hole dispersive optical model, a description of the properties of the isoscalar giant multipole resonances in one-closed-shell nuclei is proposed. Some results are compared with experimental data obtained recently for the  $^{58}\text{Ni}$ ,  $^{120}\text{Sn}$ , and  $^{142}\text{Nd}$  nuclei.

1. Gorelik M.L., Shlomo S., Tulupov B.A., and Urin M.H. // Phys. Rev. C 2021. Vol. 103, P. 034302; Phys. Rev. C 2023. Vol. 108, P. 014328.
2. Bondarenko V.I. and Urin M.H. // Phys. Rev. C 2022. Vol. 106, P. 024331; Phys. Rev. C 2024. Vol. 109, P. 064610.
3. Abdullah M., Bagchi S., Harakeh M.N., et. al. // Phys. Lett. B 2024, Vol. 855, P. 138852.

